5-15-1995

Use of fractals and kinetic equations to model thermally induced hillock formation and growth in thin metal films

Joseph Chaiken
Syracuse University

Jerry Goodisman
Syracuse University

ELSEVIER

Thin Solid Films 260 (1995) 243–251

thin Solid films

Use of fractals and kinetic equations to model thermally induced hillock formation and growth in thin metal films

J. Chaiken*, J. Goodisman

Department of Chemistry, Syracuse University, Syracuse, NY 13244-4100, USA

Received 4 May 1994; accepted 30 November 1994

Abstract

We investigated the applicability of a model based on fractals and the Smoluchowski kinetic equations to describe hillock formation in thin metal films. We have previously used this model to analyze cluster and ultrafine particle production. We show how to extract two parameters from measured hillock size distributions which may reveal the scaling of the mobility of clusters and vacancies in films with varying hillock size. On the basis of our application of this model to certain data taken from the literature, the model shows considerable potential for being able to provide an internally consistent quantitative basis for monitoring thermally driven mass redistribution processes in metal films.

Keywords: Aluminium; Annealing; Clusters; Vacancies

1. Introduction

Depending on deposition conditions, nascent metal films can have structures, i.e. "bumps", which Vook and coworkers [1, 2] called "hillocks" because of their appearance in scanning electron micrographs. The density and size distribution of these hillocks can be correlated with the temperature of the substrate during deposition and the rate at which new film material impinges on the growing film, i.e. the deposition rate. Vook and coworkers used scanning electron microscopy (SEM) to obtain hillock size distributions for a variety of Al and Al alloy films and found that annealing the films, or electromigration in such films, causes the distribution of sizes of hillocks to change. Measurements relating to the reliability of devices [3–6] composed of such films and other structures are apparently correlated with the presence and chemistry of these hillocks.

Granqvist and Buhrman [7–9] suggested that the size distribution of a collection of particles could be used to identify the particle growth mechanism [10, 11]. For example, coalescence growth [10, 11] and Ostwald ripening [12], the two most important limiting forms of particle growth in gas-to-particle conversion or grain growth in films, lead to characteristic size distributions. Coalescence growth is associated with a log-normal distribution having a longer tail to larger particle or grain size. Ostwald ripening leads to a distribution having a longer tail towards smaller sizes and a maximum particle size, consistent with the idea that there is a critical cluster or grain size below which particles are unstable with respect to the evaporation of monomers. The evaporation of monomers leads ultimately to the growth of larger clusters at the expense of those smaller than the critical size.

Vook and coworkers [1] applied the ideas of Granqvist and Buhrman and others to hillock growth in aluminum and aluminum alloy films. They concluded that for most of their data the size distributions were log-normal although there was some evidence in thermally aged samples that Ostwald ripening gains in importance. All the films studied had an oxide overlayer, and SEM secondary and backscattered electron observations suggest that hillocks are probably formed and reside on either side of, and possibly even strad-

*Corresponding author.

SSDI 0040-6090(94)06479-2

dling, this oxide layer. It is thought that, under the influence of compressive strain, atoms and small pieces of matter are forced into grain boundaries where they move towards the surface of the film away from the film–substrate interface. These atoms and small pieces of matter can coalesce with themselves and existing grains to form larger grains which may be correlated with the objects that Vook and coworkers call hillocks. The motion of the coalescing species on the grain boundaries probably involves many non-reactive interactions or collisions between coalescence events. Stated differently, hillocks diffuse from event to event rather than traveling in straight lines.

The raw data of Vook and coworkers, made available to us, consisted of sets of diameters of "bumps" in SEM images, each set containing from 50 to 215 hillocks. In this paper we reanalyze the data in terms of various population distributions including the asymptotic solution to the Smoluchowski equations describing coalescence growth. Following Vook and coworkers, we suspect that the actual mechanisms of hillock growth and particle formation are not identical and are not simple; thus it is of some fundamental interest to determine the extent to which the asymptotic solution to the Smoluchowski equations is applicable to hillock growth.

In an earlier paper [13] we showed that this asymptotic solution, which was first given by Botet and Jullien [14] in the context of cluster, particle or polymer growth, is close to the log-normal distribution. We suggested that fact [13] as the probable reason that the log-normal distribution has been used successfully for over a century to characterize empirically [15, 16] the particle size distributions. Because the systems should be conservative, in that there was effectively no loss of material from the observation zone by diffusion, the Smoluchowski model may be even more applicable to hillocks on films than to particle formation in fluid phases.

In fact, there have been two main approaches to modeling the creation and evolution of particle size distributions in thin metal films. In one approach, coalescence growth is visualized as a set of serially connected kinetic processes and the Smoluchowski equation is employed formally with random number input parameters. Applying the central limit theorem to this situation justifies usage of the log-normal distribution for the form of the particle size distribution. This approach can be quite useful because it allows calculation [17] of measurable macroscopic properties from the size distribution and the properties of the individual particles, but it is intuitively unsatisfying because there is no rigorous connection between the random number input parameters relating the microscopic properties of the coalescing entities to the parameters of the measurable particle size distribution function.

Our variation on the first approach employs the Smoluchowski equation but without using random numbers. Instead, scaling arguments are used to relate the properties of microscopic objects involved in coalescence growth to the experimentally measurable particle size distribution. The parameters obtained by fitting the solution obtained by Botet and Jullien to the experimental results reflect the fractal dimension of the trajectories of the coalescing species, the scaling of the velocities of these species with increasing size, and the dimensionality of the space in which the coalescence phenomenon occurs. The physical content of these scaling arguments, i.e. the use of so-called "fractal dimensions" (scaling exponents) remains to be fully established.

The other general approach [18, 19] involves the use of molecular dynamics or Monte Carlo simulations [20] of growth processes. Using a much more detailed description of atom diffusion [21] and the coalescence event than the Smoluchowski-equation-based methods, modeling the evolution of hillock shapes is much easier than obtaining distribution functions. Much of this type of experimental [22, 23] and theoretical work has been in the context of thin film growth or in the context of electromigration [24–26]. In these cases, there are generally many more parameters which enter into the overall physical picture than in Smoluchowski-based methods but the resulting picture is correspondingly more detailed.

In the present case, Vook and coworkers measured hillock size distributions as a function of time, which allows a test of the internal consistency of the parameters obtained from our model. This and other experiments involved alloys to which the applicability of our model has not been established. There are a variety of possible complications involving alloys. In particular, some of the alloy films that Vook and coworkers studied had stoichiometries involving more copper than is soluble in bulk pure aluminum, so that precipitates may influence the coalescence dynamics.

2. Experimental details

We were fortunate that Vook and coworkers provided us with their lists of cluster sizes. Whenever possible we use the same labels that Vook and coworkers used for the films [1] and these are indicated in Tables 1, 2 and 3. Table 1 gives data for pure aluminum films and Tables 2 and 3 pertain to copper–aluminum alloys. Vook and coworkers described their experiments adequately in earlier publications so only the most important experimental features will be provided here. All the films were evaporated onto oxidized silicon substrates according to the conditions noted in

Table 1
Table of results of fits of pure aluminum films where the film labels are the same as those used by Vook and coworkers and the processing conditions for each film are as shown

Film	Post-deposition anneal	Deposition conditions			Values of fitting parameters					
		Deposition rate (Å s^{-1})	Substrate temperature (°C)	N_{part}	a	$b \times 10^{10}$ (nm^{-3})	ln C	D	E	F
Al10	Yes	2	70	145	0.015	36.7	−14.74	185	206	79
Al11	Yes	70	250	56	−0.354	1.89	−10.79	174	129	53
Al14	Yes	70	70	99	0.488	22.0	−24.96	108	167	45
Al15	Yes	2	250	98	−0.053	3.86	−16.00	121	160	29
Al20a	No	2	70	133	0.862	412.5	−26.82	544	199	85

Table 1 and elaborated below. The careful use of backscattered and secondary electrons allowed Vook and coworkers to conclude that the hillocks were roughly hemispherical and that they were located on or just below the surfaces of the films. As deposited, all the films were of nominal total thickness 3000 Å as indicated by an in-situ crystal quartz deposition monitor (Inficon/Leybold–Heraeus).

The background pressure during deposition was one to two orders of magnitude larger than the typical pressure obtained without heating the substrate and beam source. Contamination by background gases during deposition was assumed to increase as the deposition rate decreased for a particular film thickness and background pressure. The electron microscopy counting of hillocks was done in a manner designed to avoid annealing and other effects of electron bombardment. The films were deposited in one chamber and then exposed to air as they were transferred to the scanning electron microscope for the counting of hillocks and annealing. Except for one pure aluminum film (Al20a) and one alloy film, all the films were annealed in vacuum for 1 h at 320 °C before being exposed to air and transferred to the scanning electron microscope. A set of simultaneously deposited alloy films was the subject for the thermal annealing study (Table 2). This involved heating each of the films for the stated number of minutes in high vacuum before surveying the entire film to choose a region for which the hillock size distribution was obtained. Therefore the data in the series actually correspond to different films at different times, and not to repeated observation of the same film.

3. The model

We have presented our model in detail elsewhere [13]; so we shall give only the important results. The basic idea is that the coalescence growth phenomenon can be modeled by the Smoluchowski kinetic equations [27]:

$$\frac{dn_k}{dt} = \frac{1}{2}\sum_{j=1}^{k-1} K_{j,k-j} n_j n_{k-j} - n_k \sum_{j=1}^{\infty} K_{j,k} n_j \tag{1}$$

Here, n_k is the concentration of hillocks (clusters) of size k. Botet and Jullien showed that, if the kernels $K_{i,j}$ are homogeneous, i.e.

$$K_{\lambda i,\lambda j} = \lambda^{2\omega} K_{ij} \tag{2}$$

where $2\omega < 1$, the size distribution will asymptotically approach a Poisson distribution

$$n_k \to Ck^a \exp(-bk) \tag{3}$$

regardless of the initial distribution of sizes. Here $a = -2\omega$ and b varies with time according to

$$b(t) \propto \frac{1}{2\omega - 1} \tag{4}$$

We have showed that the log-normal distribution

$$n_k = C \exp\left[-\left(\frac{\ln k + \ln c}{\sigma}\right)^2\right] \tag{5}$$

resembles the Poisson distribution over a substantial range of k.

In these equations, the value of k, referred to as the cluster size, is the number of monomers in a cluster; it is easy to show from Eq. (1) that the total monomer number $\Sigma\, kn_k$ is conserved. In applying the equations to hillock growth, something proportional to the number of atoms in a hillock should be used for k. Assuming that all hillocks have the same shape, we used the cube of the reported diameter in our analysis since volume should be proportional to the number of atoms.

As mentioned above, we have a list of observed particle diameters for each system; often, there are several particles with the same diameter. In order to avoid artifacts due to binning, we consider the cumulative number of particles of volume, i.e. diameter cubed, less than or equal to m, i.e.

$$P_m = \sum_{k=0}^{m} n_k \tag{6}$$

Table 2
Fits to Poisson distribution for films used in thermal annealing study (these films were Al–15wt.%Cu alloy films)

Time (min)	N_{part}	Σk^3	a	$b \times 10^8$ (nm^{-3})	ln C	D	E	F
18	216	8.03×10^9	1.339	6.54	−33.5	570	279	132
48	151	1.166×10^{10}	0.352	2.05	−18.8	1527	208	90
78	148	1.220×10^{10}	0.546	2.16	−22.2	2295	202	99
108	138	1.396×10^{10}	0.138	1.25	−15.73	1938	199	91
138	123	1.235×10^{10}	0.160	1.60	−15.99	2184	186	74
168	115	9.82×10^9	1.211	3.49	−33.38	1862	184	75

P_m is to be compared with the corresponding number calculated from the Poisson distribution:

$$Q_m = \int_0^m Ck^a \exp(-bk)\, dk \tag{7}$$

P_m and Q_m are evaluated at 100 equally spaced values of m, chosen for a given system by multiplying the largest volume found by 1.1 and dividing the result by 100, i.e. $m = nh$, $n = 1, \ldots, 100$. The three parameters C, a and b are chosen to minimize the r.m.s. deviation D:

$$D = \sum_{n=1}^{100} (Q_n - P_n)^2 \tag{8}$$

Because it is not possible to see and measure particles below some threshold size, the numbers of particles for smaller sizes, say diameters less than 150 nm, are subject to large uncertainties. To avoid errors from this source, we sometimes consider the "reverse cumulative number"

$$S_m = \sum_{k=m}^{\infty} n_k \tag{9}$$

This is compared with the calculated quantity

$$R_m = \int_m^{\infty} Ck^a \exp(-bk)\, dk \tag{10}$$

S_m and R_m are evaluated at the same values of m used for P_m and Q_m except that, if nh is below (150 nm)^3, the first n points are dropped in the calculation of D (Eq. (8)).

To judge whether a model fits the data for a given system, one requires a measure of the statistical errors in the data. This is obtained as follows. The number $N_m = P_m - P_{m-1}$ of particles of size between $(m-1)h$ and mh is subject to statistical fluctuation $N_m^{1/2}$, except that, if $N_m = 0$, the fluctuation is 1. Since the N_m are independent, the expected statistical error in the data is estimated as

$$E = \sum_{m=1}^{100} (M_m^{1/2})^2 \tag{11}$$

where $M_m = N_m$, or $N_m + 1$ if $N_m = 0$. Calculated values for E are given in Tables 1–3. To compare with E, we consider the corresponding deviations

$$F = \sum_{m=1}^{100} |N_m - (Q_{m+1} - Q_m)|^2$$

Calculated values for F using the distributions with optimally determined parameters are shown in the tables.

4. Results

The values of the parameters a, b and C, of the total number of particles measured and of the value of D obtained are given in Tables 1–3 for each system considered. Note that for the Poisson distribution of Table 3, the most probable size is a/b and the average size is $(a+1)/b$. If a is negative, there is no maximum in the distribution. If $a < -1$, the total particle volume is infinite.

There are essentially four types of comparison which can be made with the data provided by Vook and coworkers. First, we can compare pure aluminum films differing in deposition rate and substrate temperature, i.e. films Al10, Al11, Al14 and Al15. Comparing film Al20a with these films, the effect of the post-deposition annealing on pure aluminum films can be assessed. Another comparison can be made involving the time evolution of the hillock size distribution in Al–Cu alloy (i.e. Al–15wt.%Cu) films. Finally, the effect of increasing the proportion of Cu in the alloy is seen on comparing Al14 with Al–1.5wt.%Cu, Al–7.5wt.%Cu and Al–15wt.%Cu, after annealing for 78 min at 320 °C.

The data for the pure aluminum films are fitted quite satisfactorily by the Poisson distributions (Table 1). Fig. 1 compares the actual cumulative distribution (points) and the calculated distribution (full curve) for film Al10, which contains 145 hillocks. The broken curve shows the cumulative distribution from the best

Table 3
Fits of Poisson, log-normal and Rosin–Rammler distributions to alloy films, where A2Cu1 corresponds to (labels used by Vook and coworkers) Al–1.7wt.%Cu, A8Cu1 corresponds to Al–7.6wt.%Cu, and AcSi corresponds to Al–1.7wt.%Cu–<1wt.%Si

Distribution system	a	b (nm^{-3})	c	σ	A	C	D	E	F
Poisson distribution									
A2Cu1	−0.416	3.44×10^{-12}			1.9×10^{-5}		356	194	63
A8Cu1	−0.196	4.69×10^{-12}			1.7×10^{-7}		1130	298	76
Ac5i	0.175	2.21×10^{-12}			2.1×10^{-12}		412	153	62
Log-normal distribution									
A2Cu1			4.47×10^{-9}	0.184		2.4×10^{-9}	260	194	56
A8Cu1			2.048×10^{-8}	0.322		1.95×10^{-9}	261	298	62
AcSi			1.28×10^{-7}	0.445		1.67×10^{-10}	767	153	66
Rosin–Rammler distribution									
A2Cu1	0.764	3.28×10^{-11}				4.19×10^{-7}	1624		
A8Cu1	0.899	9.05×10^{-11}				2.29×10^{-8}	3412		
AcSi	1.094	1.48×10^{-13}				1.58×10^{-11}	431		

log-normal distribution, which gives $D = 222$, representing a slightly worse fit than the Poisson fit, $D = 185$. In Fig. 2 we compare a typical calculated distribution with a measured histogram. The average particle volume from the Poisson distribution is $(a+1)/b = 2.77 \times 10^8$ nm^3, while the log-normal distribution gives $c = 5.95 \times 10^7$ nm^3 and $\sigma = 1.488$; so the average particle size is $c \exp(3\sigma^2/4) = 3.13 \times 10^8$ nm^3, showing how similar are the log-normal and Poisson distributions. We also attempted to fit the data to the distribution corresponding to Ostwald ripening. The values of D were much larger than those obtained using the Poisson or log-normal distributions, and values of F indicated that the Ostwald distribution did not fit the experimental data.

The substrate temperature and deposition rates are extreme conditions within the working range used by Vook and coworkers. Considering the films which were subjected to the same post-deposition annealing treatment, 1 h in-situ heating at 320 °C, one can see that both films deposited at a relatively high substrate temperature (250 °C), yield negative values of the parameter a. Of these, the film with the lower deposition rate yields the larger b value. The films deposited on a colder substrate (70 °C) yeild positive values of the parameter a. Again, the film with the lower deposition rate has the larger b value.

Film Al20a was produced at exactly the same deposition conditions as film Al10 but without the post-deposition annealing treatment. Film Al20a has the most positive a and by far the largest b value of all the pure aluminum films studied. The large b value indicates an absence of large particles, suggesting that these form from smaller particles during annealing. The parameters a and b decrease with increased substrate temperature; these changes are in the same direction as the changes in a and b induced by the post-deposition annealing treatment.

We turn now to the series of alloy samples with different times of in-situ thermal annealing. The results of our analysis are given in Table 2. Fig. 3 shows the time series of Poisson distributions renormalized so that the area under each is unity. Except for the longest annealing time, the values of both the a and the b parameters became progressively smaller with increasing time. At the longest time, the a and b parameters reverted to being nearly as large as they were at 18 min annealing time. The total hillock volume, which is shown in Table 2 as Σk^3, also decreased for the longest time, approaching the value observed at 18 min. The total number of hillocks counted after annealing for 168 min was the smallest of all the times sampled and was only about half the number counted at the earliest time. Note that the measurements at different times were actually made on different films.

As indicated above, if data involving the time evolution of a hillock size distribution are available, then the value of ω can be determined from either a or b. A plot of $\ln b$ against $\ln t$ should produce a straight line with slope $1/(2\omega - 1)$. Such a plot is shown in Fig. 4 based on a and b values taken from fits of reverse cumulative numbers (Eq. (9)). Linear regression on all the data in the graph gives a correlation between $\ln b$ and $\ln t$ of $R^2 = 0.44$. If the one datum corresponding to 168 min is ignored, then a linear correlation of $R^2 = 0.94$ can be found with a slope of -1.19. This corresponds to an ω value of 0.081. The value of a is not constant across the series, as is predicted by our model. However, the average value of a across the series is -0.172 which corresponds to $\omega = 0.086$. This agrees with the value of ω obtained from b.

If we use the cumulative distributions P_m (Eq. (6)), which are subject to the effects of undercounting the smaller clusters, the results are qualitatively similar to those obtained using the reverse cumulative distribu-

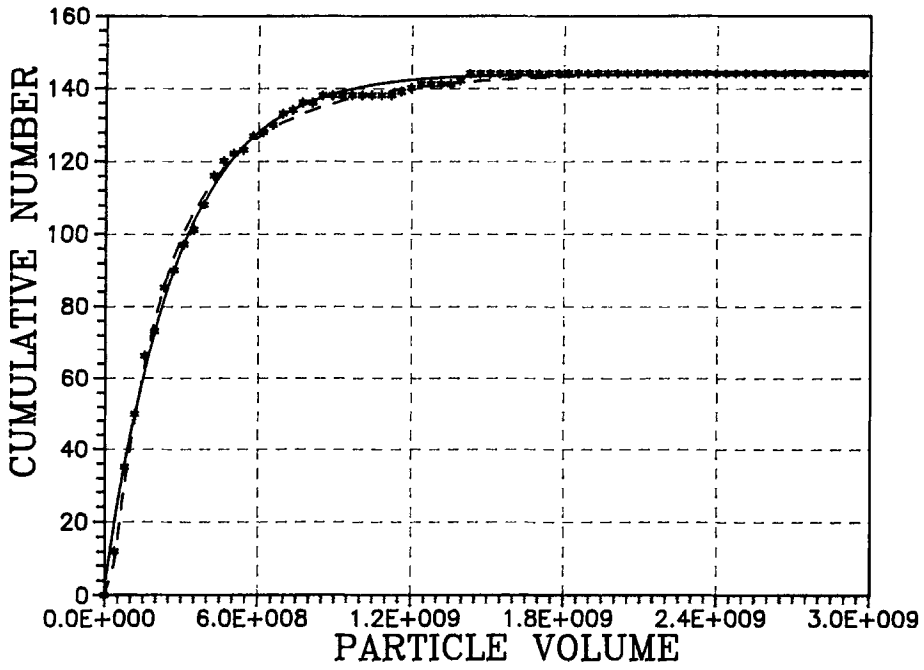

Fig. 1. Fit of film Al10 cumulative number data (*) to log-normal (– – –) and Poisson distributions (——).

tions. The a and b values for the largest time do not follow the trend of the others. Dropping this point, we perform linear regression on $\ln b$ vs. $\ln t$, obtaining $R^2 = 0.87$ and a slope of -0.73, which yields $\omega = -0.18$. This compares reasonably well with the ω calculated from the average value of a for the first five points: $a = 0.51$; $\omega = -0.25$.

Varying the composition of the alloy film produced substantial effects on the distributions. Turning from the distribution produced in the pure film Al14 to that produced in Al–1.5wt.%Cu, which had the same post-deposition annealing treatment as all the annealed pure aluminum films, we find that the a parameter became negative and the b parameter decreased by roughly three orders of magnitude. Increasing the proportion of copper further, while maintaining the same post-deposition annealing treatment (Al–7.5wt.%Cu), the a parameter became less negative and the b parameter was not changed substantially. However, it should be noted that a film having nearly double the proportion of copper but deposited at a much lower substrate temperature (a factor of 3 lower than that for all the other films used in this comparison) and only 10% larger deposition rate, Al–15wt.%Cu, had an a parameter roughly comparable with that of the pure aluminum film and a b parameter four orders of magnitude larger than either of the lower proportion copper alloy films.

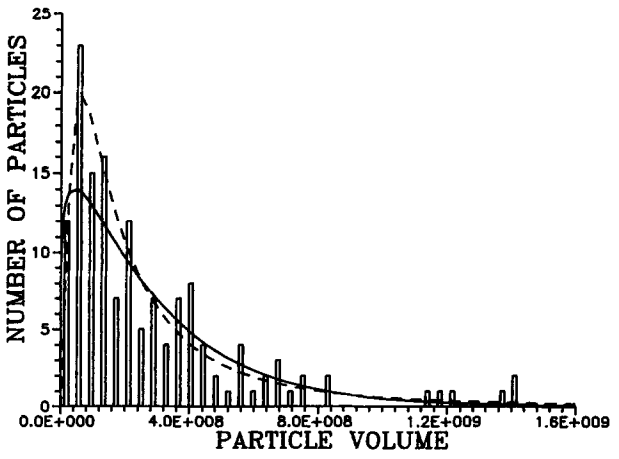

Fig. 2. Poisson and log-normal distributions for film Al10 data compared with histogram of volumes.

With regard to the relative suitability of the Poisson, Rosin–Rammler and log-normal distributions to represent the hillock size distributions, we compare values of D, for which differences are far more apparent than for F. For the first two alloy films, the log-normal distribution is significantly better than the Poisson distribution, although $F < E$ in all cases, but the reverse is true for the third alloy. The Rosin–Rammler distribution is far inferior to the other two for the first two alloys, but comparable with the Poisson distribution, which has the lowest D of the three distributions, for the third. Almost always the distributions for the pure aluminum films are better represented using the Poisson distribution and those for the alloy films are better represented using the log-normal distribution. For the time evolution experiment, which involves alloys, the data were best represented using the log-normal distribution. The Ostwald ripening distribution (results not shown) was far inferior to the others for all samples.

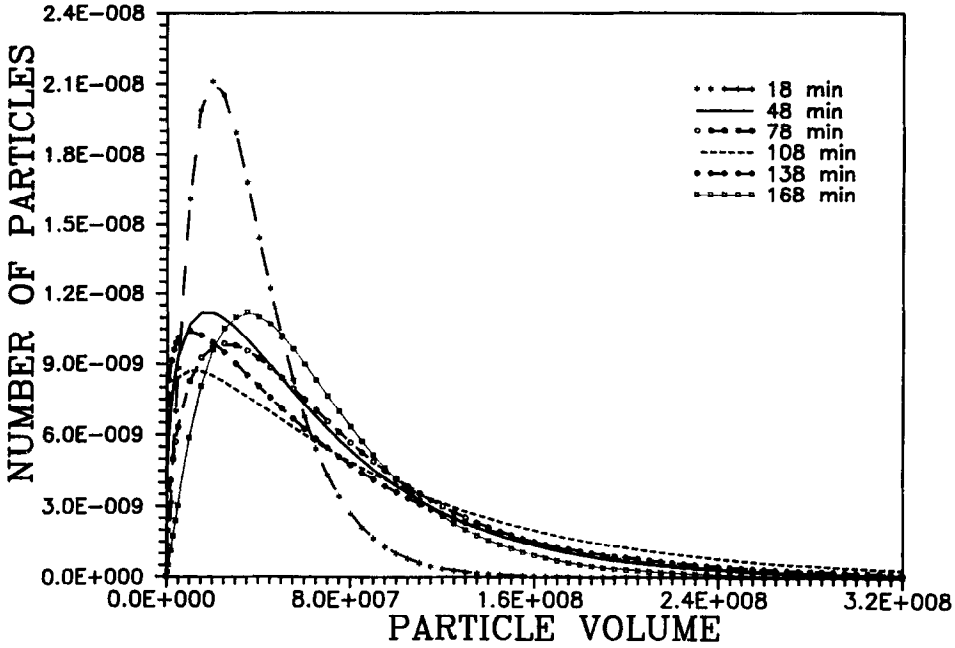

Fig. 3. Best Poisson distributions for films of thermal annealing study; all are normalized to unit area.

5. Discussion

In the Poisson distribution for population as a function of cluster size, the value of a is most sensitive to the behavior for small sizes and the value of b most sensitive to the behavior for larger sizes. One expects a large positive value of a for distributions with a steep leading edge. A negative value of a in the Poisson distribution leads to a distribution which is decreasing for all values of the cluster size, i.e. it is not a peaked distribution. The value of b determines how fast n_k approaches zero with increasing k. A sharply peaked distribution would require a large positive value for b to give the short tail to large sizes.

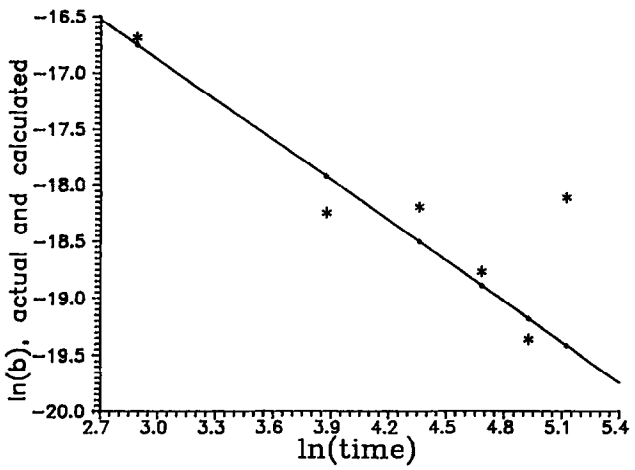

Fig. 4. Linear fit to $\ln b$ vs. $\ln t$ values (*) obtained from thermal annealing study.

The detection sensitivity, i.e. counting efficiency, for clusters and hillocks smaller than a certain size is zero. Vook and coworkers considered the smallest hillock size sufficiently visible by SEM and well defined to be included in the count as ≈ 0.15–$0.20\,\mu m$. In many cases, the apparent shape of the distribution on the side to smaller sizes than the maximum is mostly fixed by the bin width and the value of the minimum hillock size which can be observed. This is seen in Figs. 1 and 2, for example. Whenever a negative value was obtained, it was found that D, the sum of squares of residuals, involved very few data points from the small-size side of the distribution. In addition, the Poisson distribution is thought to hold particularly well at large cluster and hillock sizes.

The apparent value of a may change during the growth of a distribution of hillocks because in the small regime, corresponding to short evolution times, the shape of the distribution is determined by the dependence of detection sensitivity on hillock size. At later times, when the distribution has shifted to larger sizes, the value of a approaches that resulting from the actual shape of the hillock size distribution. Thus the value of b should be considered to be more reliably determined by the data whereas the a parameter is more susceptible to systematic error. The variation in the b parameter with time in the series in Table 2 is roughly as expected.

Because our model has sufficient flexibility and the basic features needed to model the kinetics of hillock formation and growth, we suggest that much of what is observed in the SEM studies can be explained physically in terms of the coalescence growth kinetics, the

mass transfer conditions and the scaling properties of these processes. What is needed to test the model more clearly is a similar experiment utilizing pure metals, ideally with and without the influence of any oxide coatings. At present, the values of the parameters obtained from the data are physically reasonable, given the effects of finite sample size.

We now consider our results in terms of underlying physical mechanisms. The pure aluminum film which was not annealed, Al20a, had a very sharp distribution and consequently had a relatively large positive a and the largest b parameter of all the pure aluminum distributions measured. On annealing, a film deposited under identical conditions evolved into a broader distribution with larger hillocks; a became substantially less positive and b became smaller by an order of magnitude. Both of these films were deposited at a relatively cold substrate temperature and slow deposition rate. Increasing the deposition rate and/or the substrate temperature during deposition has the same qualitative effect on the parameters as annealing a film after deposition is complete; so it may be that all three changes act in the same way.

The equivalence between substrate temperature and post-deposition annealing is obvious. Increasing substrate temperature, during or after deposition, increases the rate of mass transfer and supplies activation energy needed for nascent hillocks to reorganize internally. Vook and coworkers suggested that decreasing the deposition rate increases the amount of background gases incorporated into the film, promoting nucleation in and on the growing film during deposition and producing more and smaller particles. However, nucleation can be initiated by density fluctuations; so background gases are not needed for either film or particle growth. To understand the equivalence of deposition rate, we note that a small local temperature rise on and in the growing film is produced by the impinging material. In the case of aluminum, the source is a wire basket which is white hot, $\approx 1600\,^{\circ}\mathrm{C}$. Thus the average substrate temperature should increase with increasing deposition rate, resulting in coalescence growth of various mobile entities to form larger, less mobile entities.

This analysis suggests an experiment which could help to unravel the explanation of the dependence of hillock size distribution on deposition rate. The deposition rate can be varied either by changing the heating power causing the evaporation of the source material or by varying the distance between the source and the substrate, since there is an inverse-square dependence of the density of a molecular or atomic beam on the distance from the source of that beam. If the behavior of the hillock size distribution depends on the incorporation of background gases, a shift towards smaller clusters should result from moving the substrate closer to the source. If there is a local heating effect, as we have suggested, the distribution should shift towards larger sizes as the substrate is placed closer to the beam source.

A positive a parameter corresponds to a negative scaling parameter ω and a peaked hillock size distribution. Scaling is thought to be valid for $\omega \leqslant \frac{1}{2}$, and ω is related to physical attributes and chemical mechanisms by

$$2\omega = \alpha + \frac{d - d_w}{D} \tag{12}$$

In the context of hillock growth by mass-transfer-limited coalescence, α describes how the speed of movement of material associated with a hillock decreases with increasing hillock volume. Its value would be $-\frac{1}{2}$ if all the hillocks had the same kinetic energy, as in the gas phase. The parameter D is the fractal dimension of the hillocks, depending on how the mass of the hillock is distributed in space; d is the dimension of the space in which the coalescence process occurs and would be 2 if hillock and vacancy motion [28] in and around grain boundaries is mostly responsible for coalescence growth. The parameter d_w is the fractal dimension of the trajectories of the coalescing species between coalescence events and would be 2 for diffusive mass transport. With these values of the parameters, $\omega = \alpha/2 = -0.25$.

Of the values of a and ω obtained for the pure aluminum films, only that for film Al20a does not reflect post-deposition annealing. The value for ω, -0.43, suggests that the mobility of hillocks decreases more rapidly with increasing hillock size than for cluster translation in the gas phase, for which the mobility decreases simply because the mass increases ($\alpha = -\frac{1}{2}$). We hypothesize that larger hillocks are slowed down because the number of atoms on its surface which can interact with the environment increases. This number grows as the $\frac{2}{3}$ power of the number of atoms in a hillock.

6. Conclusions

The coalescence growth of hillocks in thin films can be quantitatively modeled using the Smoluchowski equation. The distribution of hillock sizes in either nascent films or pre-deposited films which undergo thermal processing can be represented by a Poisson distribution function. The model explains the parameters in the distribution in terms of an underlying collision mechanism and the geometry of the motion and space in which the coalescence occurs. For an isothermal system, the slowing down of the motion of hillocks as they become larger seems to be the main determinant of the actual shape of measured distributions.

Acknowledgments

We would like to thank Professor R. W. Vook and coworkers for the use of their data and for some useful conversations.

References

[1] S. Aceto, C. Y. Chang and R. W. Vook, *Thin Solid Films, 219* (1992) 80–86.
[2] C. Y. Chang and R. W. Vook, *J. Vac. Sci. Technol. A, 9* (1990) 559–562.
[3] C. Y. Chang and R. W. Vook, *Materials Reliability Issues in Microelectronics, Materials Research Society Symp. Proc.*, Vol. 225, Materials Research Society, Pitsburgh, PA, 1991, pp. 125–129.
[4] C. Y. Chang and R. W. Vook, *Appl. Surf. Sci., 60–61* (1992) 71–78.
[5] C. Y. Chang and R. W. Vook, *Thin Solid Films, 223* (1993) 23–30.
[6] R. W. Vook, *Mater. Chem. Phys., 36* (1994) 199–216.
[7] C. G. Granqvist and R. A. Buhrman, *J. Catal., 42* (1976) 477.
[8] C. G. Granqvist and R. A. Buhrman, *Solid State Commun., 18* (1976) 123–126.
[9] C. G. Granqvist and R. A. Buhrman, *Appl. Phys. Lett., 27* (1975) 693–694.
[10] P. Wynblatt and N. A. Gjostein, *Prog. Solid State Chem., 9* (1975) 21–58.
[11] I. Vavra and S. Luby, *Czech. J. Phys. B, 30* (1980) 175.
[12] I. M. Lifschitz and V. V. Slyozov, *Phys. Chem. Solids, 19* (1961) 35–50.
[13] M. Villarica, M. J. Casey, J. Goodisman and J. Chaiken, *J. Chem. Phys., 98* (1993) 4610–4625.
[14] R. Botet and R. Jullien, *J. Phys. A, 17* (1984) 2517–2530.
[15] I. Pocsik, *Z. Phys. D, 20* (1991) 395–397.
[16] J. Chaiken, M. J. Casey and R. M. Villarica, *J. Phys. Chem., 96* (1992) 3183–3186.
[17] C. G. Granqvist and R. A. Buhrman, *J. Appl. Phys., 47* (1976) 2220–2222.
[18] M. C. Bartlett and J. W. Evans, *Surf. Sci., 314* (1994) L829–L834.
[19] M. C. Bartlett and J. W. Evans, *Surf. Sci., 314* (1994) L835–L842.
[20] P. Smilauer, M. R. Wilby and D. D. Vvedensky, *Phys. Rev. B, 47* (1993) 4119–4122.
[21] P. J. Feibelman, *Phys. Rev. Lett., 65* (1990) 729–732.
[22] R. Kunkel, B. Poelsema, L. K. Verheij, G. Comsa, *Phys. Rev. Lett., 65* (1990) 733–736.
[23] R. Q. Hwang and R. J. Behm, *J. Vac. Sci. Technol. B, 10* (1992) 256–261.
[24] G. O. Ramseyer, J. V. Beasock, L. H. Walsh and W. K. Sylla, *Materials Research Society Symp Proc.*, Vol. 318, Materials Research Society, Pittsburgh, PA, 1994, pp. 329–334.
[25] G. O. Ramseyer, L. H. Walsh, J. V. Beasock and T. E. Renz, *Materials Research Society Symp. Proc.*, Materials Research Society, Pittsburgh, PA, 1994, Vol. 338, 1994, pp. 421–426.
[26] Y. J. Kime and P. Grach, *Materials Research Society Symp. Proc.*, Materials Research Society, Pittsburgh, PA, 1994, Vol. 338, 1994, pp. 255–260.
[27] M. V. Smoluchowski, *Phys. Z., 17* (1916) 585.
[28] E. E. Gruber, *J. Appl. Phys., 38* (1967) 243–250.